Monte Carlo Simulation of a Coarse-Grained Model of Polyelectrolyte Networks

Qiliang Yan and Juan J. de Pablo*

Department of Chemical Engineering, University of Wisconsin–Madison, Madison, Wisconsin 53706, USA

(Received 3 December 2002; published 3 July 2003)

The structure and properties of a coarse-grained model of a polyelectrolyte network is studied by means of Monte Carlo simulations. Counterions are treated explicitly, and permanent tetrafunctional cross-linking sites are annealed. The resulting pressure-density relationships exhibit a strong dependence on the strength of electrostatic interactions. A discontinuous volume change is observed when electrostatic interactions are strong. The structure of the model networks is examined at various conditions, and it is found to be considerably different from that of noncross-linked polyelectrolytes.

DOI: 10.1103/PhysRevLett.91.018301 PACS numbers: 82.35.Rs, 61.41.+e, 64.10.+h, 64.75.+g

Polyelectrolyte gels have a network structure consisting of cross-linked polymer chains with charged groups and counterions. When a dry polyelectrolyte gel is immersed in a solvent, it can absorb large amounts of solvent and expand its volume considerably. It is also experimentally observed that charged gels can undergo a discontinuous volume transition under certain solvent conditions [1–3]. This unusual but controllable volume behavior has led to numerous uses of polyelectrolyte gels, including applications in drug delivery, environmental cleanup operations (as superabsorbent materials), and microfluidic devices (as actuators).

Recent theoretical work on polyelectrolytes has increased our understanding of these systems considerably [4–6]; furthermore, molecular simulations have helped us assess some of the approximations invoked in various theoretical treatments [7–10]. Much less theoretical and numerical work has been conducted on *cross-linked* polyelectrolytes or gels.

In recent years, molecular simulations of simple electrolyte and colloidal models have revealed that ionic association in such systems leads to unexpected behaviors and trends, some of which are not captured by bare integral-equation formalisms [11–13]. We believe that for the more complex case of charged polyelectrolyte gels, molecular simulations could also help clarify the current understanding of this important class of materials. Note that simulation reports on the structure and properties of *neutral* polymeric networks have shed considerable light into the behavior of elastomers [14–17]. However, with one exception [16], *direct* observations of first-order phase transitions in such networks have remained elusive [17]. Perhaps more importantly, most literature studies have been restricted to study of *neutral* polymeric networks. An earlier account of a charged polymeric network was limited to a two-dimensional system on a lattice and in the absence of explicit counterions [18]. Very recently, Schneider and Linse [19] have presented simulations of relatively small samples of polyelectrolyte gels.

In this Letter we present the results of simulations of large polyelectrolyte networks in the presence of explicit counterions. The goals of our work are twofold. Discontinuous volume transitions are experimentally observed when weakly charged gels are placed in a poor solvent. In this work, we first seek to determine whether a model consisting of a charged polymeric network and explicit counterions is sufficient to generate a first-order swelling transition analogous to that observed experimentally in some types of gels. Second, we seek to determine the molecular structure of the gel in the swollen and collapsed states, thereby providing exact numerical data to assess the validity of some of the assumptions implicit in theoretical treatments.

The system considered in this work consists of a perfect, defect-free network of polymer chains connected at the ends to tetrafunctional cross-linking sites (nodes). Our simulation system consists of $N_{\text{node}} = 64$ nodes and $N_{\text{chain}} = 128$ cross-linked chains. All polymer chains consist of $n = 98$ monomers. Both monomers and nodes carry a unit negative charge $z = -1$. The total number of particles on the network backbone is $N_{\text{node}} \times (2n + 1) = 12\,608$. An equal number of monovalent counterions is included in the simulation. The solvent is treated implicitly as a dielectric continuum.

Polymer chains are modeled as a sequence of charged soft spheres connected by finite extensible nonlinear elastic (FENE) springs. The total potential energy of the system includes three contributions: van der Waals (Lennard-Jones) interactions between nonbonded particles, Coulombic interactions between charged sites, and permanent bonds between adjacent monomers. Lennard-Jones interactions between nonbonded sites are cut off at $r_c = 2^{1/6}$ and are purely repulsive (polymer chains are immersed in a good solvent). In this work, all particles have the same diameter σ and energy parameter ϵ. Throughout this work, the reduced temperature $T^* = \epsilon/k_B T$ is set to 1.

The bonding energy between adjacent monomers is described by a FENE potential energy function

$$U^{\text{bond}}(r) = -\frac{1}{2} K_{\text{bond}} R^2 \ln\left[1 - \left(\frac{r}{R}\right)^2\right], \qquad (1)$$

where K_{bond} is the spring force constant, and R is the

maximum bond length. Throughout this work we use $K_{\text{bond}} = 10k_{\text{B}}T$, and $R = 1.5\sigma$.

The Coulombic energy of interaction is given by

$$U^{\text{elec}}(r_{ij}) = k_{\text{B}}T\frac{z_i z_j \lambda}{r_{ij}}, \tag{2}$$

where the Bjerrum length λ is defined as the distance at which two unit charges have interaction energy $k_{\text{B}}T$, i.e.,

$$\lambda = \frac{e^2}{4\pi\epsilon_0\epsilon k_{\text{B}}T}, \tag{3}$$

where ϵ is the dielectric constant of the solvent. The Bjerrum length is one of the key parameters considered in this work, as it provides a measure of the strength of electrostatic interactions *vis à vis* the thermal energy of the system.

A finely discretized lattice is employed to improve the performance of the simulations and to facilitate the study of large simulation systems [20]. In this work, the diameter σ of a particle is divided into $\xi = 6$ lattice units. It has been shown that this discretization level provides a faithful approximation of the original, continuum model system. The long-range Coulomb interaction is calculated by the Ewald sum method with conducting boundary conditions.

The Monte Carlo simulations presented here are conducted in the canonical ensemble. Trial configurations are generated by simple monomer displacements and by extended continuum configurational bias moves [21–24]. In the latter moves, a portion of a polymer chain (usually two to three beads) is first deleted, resulting in 2 (or 4, if a node is involved) open ends. These open ends are then reconnected again by regenerating the missing portion of the chain using configurational bias techniques. A self-adaptive weighting function is used to guide the regeneration process [24].

The osmotic pressure of the system is calculated from the virial equation, $p = \rho k_B T + W/V$, where the internal virial W is calculated from the sum of a pair virial function $w(r_{ij}) = r_{ij}\, dU(r_{ij})/d\, r_{ij}$. Figure 1 shows the osmotic pressure as a function of the packing fraction for different values of the Bjerrum length, where the packing fraction is defined as $\eta = (N_{\text{node}} + nN_{\text{chain}})\sigma^3/V$. The largest statistical uncertainties in osmotic pressure calculations (corresponding to the highest density and largest Bjerrum length) are approximately 0.02. The pressure becomes negative at sufficiently small packing fractions, where elastic contributions to the free energy dominate the behavior of the network (the low-density limit of this network, when it is fully stretched, is $\eta = 0.000\,31$). The pressure-density relationship shows a strong dependence on the Bjerrum length (or the strength of electrostatic interactions). At small Bjerrum lengths, which imply either a solvent with a high dielectric constant or a high concentration of added salts, the osmotic pressure is a monotonically increasing function of density. The curve crosses the zero-pressure line at a small packing fraction,

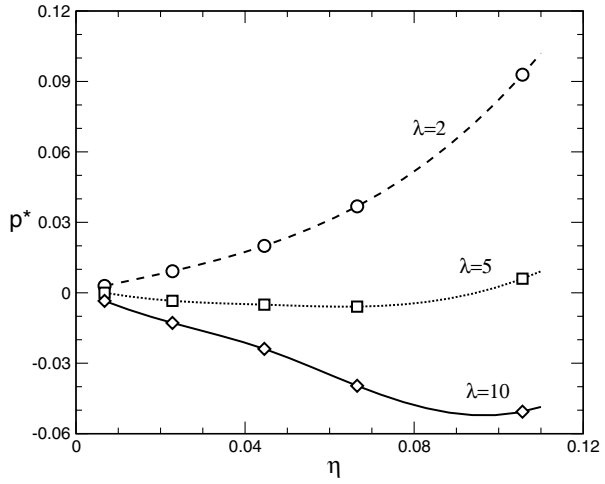

FIG. 1. Osmotic pressure of model polyelectrolyte gels as a function of packing fraction. Circles are data for Bjerrum length $\lambda = 2$, squares are data for $\lambda = 5$, and diamonds are data for $\lambda = 10$. The lines are drawn as a guide to the eye.

indicating that the gel is highly swollen. As the Bjerrum length is increased, the pressure curve starts to develop an unstable region, and crosses zero at two points: one at a low packing fraction and one at a higher packing fraction, implying the onset of a first-order phase transition. At large Bjerrum lengths, the "S" shaped loop of the curve becomes pronounced, and the isotherm crosses zero only at high packing fractions, indicating that the gel collapses.

We next proceed to examine the structure of the gel along the two branches of the coexistence curve. For $\lambda = 5$, these branches correspond approximately to $\eta = 0.0067$ and $\eta = 0.106$. Figure 2 shows the single-chain structure factor of a gel for $\lambda = 5$ at packing fraction $\eta = 0.106$. As the osmotic pressure data imply, the gel at these conditions is collapsed. In the high k region ($kR_g \gg 1$), the structure factor scales as $S(k) \propto k^{-1/\nu}$, where ν is the Flory exponent. This figure indicates that polymer strands inside a collapsed network exhibit two distinct scaling regimes: in the region $1 < k < 4$, the structure factor scales as $S(k) \propto k^{-1}$, which suggests that at short distances chains are highly extended. This is mainly due to the electrostatic repulsion between charged monomers. At longer length scales, in the region $0.3 < k < 0.6$, the structure factor scales as $S(k) \propto k^{-3}$, indicating that, globally, chains adopt a tight globular conformation. These two extremes of chain conformation coexist in the same system. Figure 2 also shows the structure factor of an uncross-linked polyelectrolyte solution at the same conditions. At short length scales the uncross-linked polyelectrolyte chains exhibit the same Flory exponent as the gel does; at longer length scales, however, the uncross-linked polyelectrolyte chains are almost Gaussian and not as globular as in the gel.

Figure 3 shows the structure factor of a swollen gel at $\lambda = 5$ and $\eta = 0.0067$. Under these conditions the

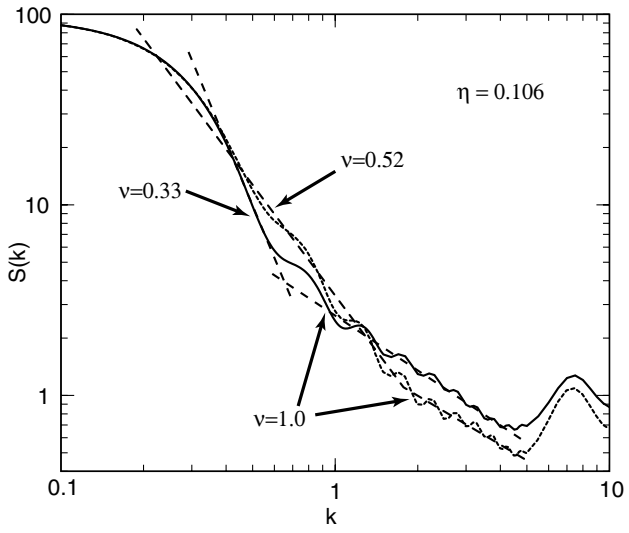

FIG. 2. Structure factor of a collapsed gel and a polyelectrolyte solution for $\lambda = 5$ at the same packing fraction $\eta = 0.106$. The solid curve is the result for gel; the dotted curve is the result for an uncross-linked polyelectrolyte solution.

system exhibits a uniform scaling behavior; the scaling exponent is $\nu = 0.72$, indicating that the conformations of polymer chains in a swollen gel are slightly more expanded than those for a single chain in a good solvent. The exponent found in this case is consistent with that reported for a neutral polymeric gel [15]. Interestingly, the structure factor of uncross-linked polyelectrolyte chains under these conditions is almost the same as that for a packing fraction $\eta = 0.106$. This density-independent behavior can be explained by the fact that for $\lambda = 5$, uncross-linked polyelectrolytes start to form aggregates; increasing the packing fraction only increases the number of aggregates in the system, but not the structure of each aggregate. This behavior is different from that reported by Stevens and Kremer [7] for uncross-linked polyelectrolytes at lower values of λ ($\lambda = 0.833\sigma$, to be precise).

In the counterion condensation framework proposed by Manning and Oosawa [6,25,26], counterions are anticipated to form a thin condensation layer around the surface of polyelectrolyte molecules when the Bjerrum length exceeds the so-called Manning critical value. To interpret our results in the context of condensation theory, we analyze the counterion-counterion pair distribution; if counterions form a permanent condensed layer on the surface of the polyelectrolyte, these condensed counterions should exhibit long-range correlations due to the connectivity of the polymer. Figure 4 shows the counterion-counterion pair distribution function for three different values of Bjerrum length. For $\lambda = 1$, this function increases monotonically with distance and approaches unity around $r = 3\sigma$, indicating that no counterion condensation occurs. For $\lambda = 2$, the function increases at short distances, and exceeds 1 at $r = 2$. The function remains slightly above unity even at distances as large as $r = 10$; this broad peak suggests that counterion condensation starts to occur at $\lambda = 2$. For $\lambda = 5$, the distribution function shows a pronounced peak around $r = 2.1\sigma$, and extends over long distances, indicating a pronounced degree of condensation.

Figure 5 shows nonbonded monomer-monomer pair distribution functions for several Bjerrum lengths. At small distances ($r < 1.5\sigma$), the pair distribution decreases as the Bjerrum length increases. This is expected because the electrostatic repulsion becomes stronger. More interestingly, at short distances the pair distribution functions for $\lambda = 5$ and $\lambda = 10$ are almost the same, while they

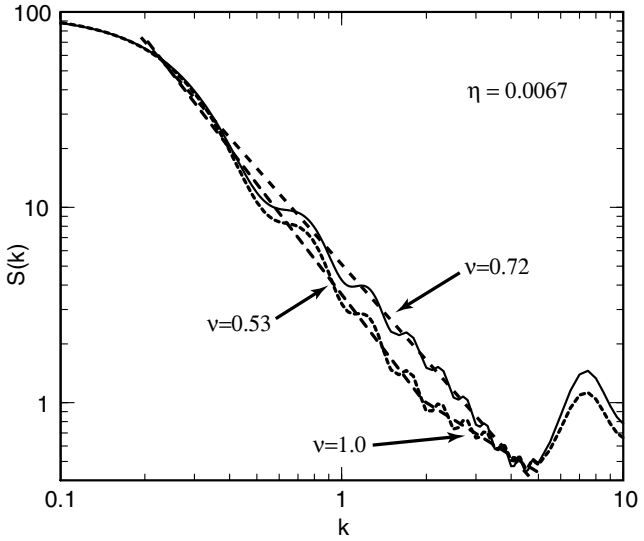

FIG. 3. Structure factor of a swollen gel and a polyelectrolyte solution for $\lambda = 5$ at the same packing fraction $\eta = 0.0067$. The symbols are the same as in Fig. 2.

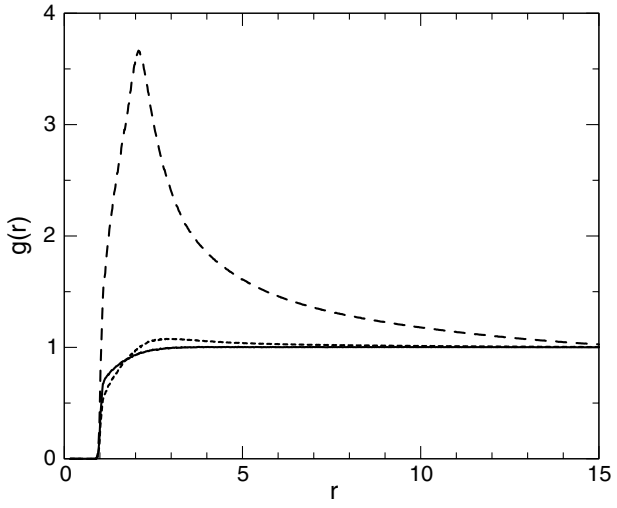

FIG. 4. Counterion-counterion pair distribution functions for gels at $\eta = 0.0067$, with various Bjerrum lengths. The solid line is for $\lambda = 1$, the dotted line is for $\lambda = 2$, and the dashed line is for $\lambda = 5$.

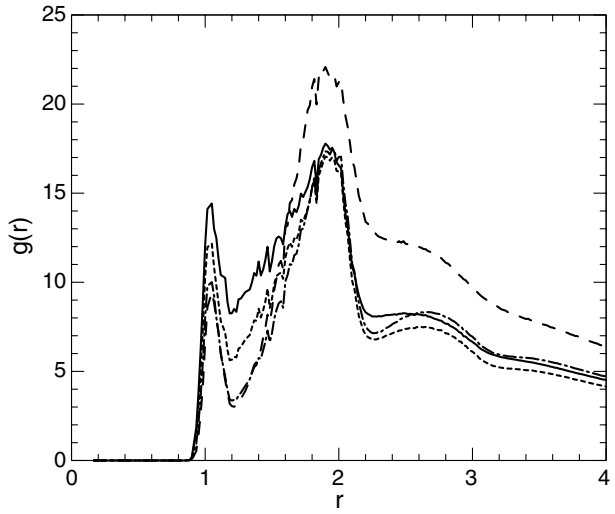

FIG. 5. Monomer-monomer pair distribution functions for gels at $\eta = 0.0067$, with various Bjerrum lengths. The solid line is for $\lambda = 1$, the dotted line is for $\lambda = 2$, the dash-dotted line is for $\lambda = 5$, and the dashed line is for $\lambda = 10$.

change considerably when λ increases from 1 to 5. This is consistent with the charge renormalization anticipated in counterion condensation theory.

At large distances ($r > 2\sigma$), these distribution functions change in a different manner when the Bjerrum length increases. The distribution function decreases only slightly when the Bjerrum length changes from 1 to 2. However, when the Bjerrum length increases farther, the distribution function also *increases*. This increase is pronounced for $\lambda = 10$. This unusual behavior indicates that monomers, which carry like charges, start to effectively *attract* each other at long distances whenever the Bjerrum length is larger than 2. The onset of this effective attraction coincides with the condensation of counterions; we attribute its origins to the bridging effect and the strong correlations between charges resulting from counterion condensation. Note that recent theories [27–30] do predict an attractive interaction between uncross-linked polyelectrolyte chains. Given the fact that gels start to exhibit a discontinuous volume change at $\lambda = 5$, it is proposed that this effective attraction between monomers is eventually responsible for the collapse of polyelectrolyte gels observed in our model.

In summary, our simulations have shown that a model consisting of a charged polymer network and explicit counterions is sufficient to give rise to a first-order swelling transition. In the collapsed state, polymer strands inside the gel exhibit two scaling exponents: at short distances, chains are completely extended, and at long distances chains are globular. In the swollen state, network strands exhibit a single scaling exponent and are extended beyond good solvent statistics. We find that counterion-mediated interactions lead to effective attractions between network strands of like charge, eventually giving rise to the collapse of a gel at sufficiently low salt concentrations.

This work was supported by the National Science Foundation (CTS-0218357).

*Electronic address: depablo@engr.wisc.edu

[1] T. Tanaka, D. Fillmore, S. T. Sun, I. Nishio, G. Swislow, and A. Shah, Phys. Rev. Lett. **45**, 1636 (1980).
[2] S. Panyukov and Y. Rabin, Macromolecules **29**, 8530 (1996).
[3] *Advanced Polymer Science*, edited by K. Dusek (Springer-Verlag, Tokyo, 1993), Vols. 109–110.
[4] L. Blum, J. Phys. Condens. Matter **8**, A143 (1996).
[5] M. Muthukumar, J. Chem. Phys. **105**, 5183 (1996).
[6] G. S. Manning and J. Ray, J. Biomol. Struct. Dyn. **16**, 461 (1998).
[7] M. J. Stevens and K. Kremer, J. Chem. Phys. **103**, 1669 (1995).
[8] U. Micka, C. Holm, and K. Kremer, Langmuir **15**, 4033 (1999).
[9] T. Wallin and P. Linse, Langmuir **12**, 305 (1996).
[10] M. Jonson and P. Linse, J. Chem. Phys. **115**, 3406 (2001).
[11] P. Linse, Philos. Trans. R. Soc. London, Ser. A **359**, 853 (2001).
[12] A. Z. Panagiotopoulos and M. E. Fisher, Phys. Rev. Lett. **88**, 045701 (2002).
[13] Q. Yan and J. J. de Pablo, Phys. Rev. Lett. **88**, 095504 (2002).
[14] G. S. Grest, M. Putz, R. Everaers, and K. Kremer, J. Non-Cryst. Solids **274**, 139 (2000).
[15] M. Pütz, K. Kremer, and R. Everaers, Phys. Rev. Lett. **84**, 298 (1999).
[16] F. A. Escobedo and J. J. de Pablo, Mol. Phys. **90**, 437 (1997).
[17] F. A. Escobedo and J. J. de Pablo, Phys. Rep. **318**, 85 (1999).
[18] D. P. Aalberts, J. Polym. Sci. B **34**, 1127 (1996).
[19] S. Schneider and P. Linse, Eur. Phys. J. E **8**, 457 (2002).
[20] A. Z. Panagiotopoulos and S. K. Kumar, Phys. Rev. Lett. **83**, 2981 (1999).
[21] J. J. de Pablo, M. Laso, and U. W. Suter, J. Chem. Phys. **96**, 6157 (1992).
[22] F. A. Escobedo and J. J. de Pablo, J. Chem. Phys. **104**, 4788 (1996).
[23] Z. Chen and F. A. Escobedo, J. Chem. Phys. **113**, 11 382 (2000).
[24] C. D. Wick and J. I. Siepmann, Macromolecules **33**, 7207 (2000).
[25] G. S. Manning, J. Chem. Phys. **51**, 924 (1969).
[26] F. Oosawa, Biopolymers **6**, 1633 (1968).
[27] V. A. Bloomfield, Curr. Opin. Struct. Biol. **6**, 334 (1996).
[28] N. Gronbech-Jessen, R. J. Mashl, R. F. Bruinsma, and W. M. Gelbart, Phys. Rev. Lett. **78**, 2477 (1997).
[29] J. Ray and G. S. Manning, Macromolecules **33**, 2901 (2000).
[30] A. Y. Grosberg, T. T. Nguyen, and B. I. Shklovskii, Rev. Mod. Phys. **74**, 329 (2002).